



Original Article

Long noncoding RNA LOC441461 drives cancer growth and is associated with poor clinical outcomes

Ching-Feng Cheng^{a,b}, Ya-Ting Tu^c, Yi-Ru Chen^c, Ming-Cheng Lee^c, Hui-Chen Ku^d, Kuo-Wang Tsai^{c,d*}

^aDepartment of Pediatrics, Taipei Tzu Chi Hospital, Buddhist Tzu Chi Medical Foundation, Taipei, Taiwan, ^bSchool of Medicine, Tzu Chi University, Hualien, Taiwan, ^cDepartment of Research, Taipei Tzu Chi Hospital, Buddhist Tzu Chi Medical Foundation, Taipei, Taiwan, ^dDepartment of Nursing, Cardinal Tien Junior College of Healthcare and Management, Taipei, Taiwan

Submission : 06-Jul-2025
Revision : 08-Aug-2025
Acceptance : 08-Sep-2025
Web Publication : 13-Jan-2026

ABSTRACT

Objectives: The role of LOC441461, a long noncoding RNA, differs in different cancer types, and its role in lung cancer remains unclear. **Materials and Methods:** We investigated the clinical significance of LOC441461 expression in lung cancer using bioinformatics analyses. To explore the biological function of LOC441461, we performed siRNA-mediated knockdown in lung cancer cells and evaluated its effects on cell proliferation, colony formation, apoptosis, and cell cycle progression. **Results:** LOC441461 was found to be significantly overexpressed in lung adenocarcinoma (LUAD), and LOC441461 overexpression was significantly associated with poor prognosis in patients with LUAD. LOC441461 knockdown significantly inhibited cell growth and induced a modest but statistically significant increase in apoptosis in lung cancer cells. According to a cell cycle analysis, LOC441461 knockdown induced G0/G1 arrest in A549 cells; increased p21 and p27 expression; and reduced the levels of CDK4 and the cyclins A2, B1, and D1, similar to p53-dependent regulation. By contrast, H1299 cells exhibited G2/M accumulation with no change in p21 and p27 levels, suggesting a p53-independent mechanism. **Conclusion:** Our findings indicate that high LOC441461 expression is correlated with worse prognosis in LUAD. These results support the potential of LOC441461 as a novel therapeutic and prognostic target in LUAD.

KEYWORDS: *lncRNA, LOC441461, Lung cancer*

INTRODUCTION

Lung cancer is primarily driven by genetics and environmental exposure, whether through pollution, radiation, or tobacco consumption [1]. It remains the leading cause of cancer-related deaths worldwide, with over 40% of cases of nonsmall-cell lung cancer (NSCLC) already metastatic at the time of diagnosis [2]. Most patients with NSCLC receive a diagnosis at an advanced stage, resulting in a low clinical cure rate of approximately 15%. The two major histological subtypes of NSCLC are lung adenocarcinoma (LUAD) and lung squamous cell carcinoma (LUSC). Lung cancer cells are frequently involved in key cancer-associated pathways related to cell proliferation, programmed cell death, angiogenesis, invasion, and metastasis [3]. The transformation of normal lung epithelial cells into malignant cells is thought to occur over multiple steps involving both genetic and epigenetic alterations, leading to clonal expansion and invasive disease [4].

Evidence suggests that noncoding RNAs play a

critical role in cancer biology, including the development, progression, metastasis, and drug resistance of tumors [5]. Long noncoding RNAs (lncRNAs), which are RNA transcripts longer than 200 nucleotides, have been shown to participate in several regulatory mechanisms; they (1) modulate protein-coding gene expression, (2) alter epigenetic regulation, (3) influence alternative splicing, and (4) act as decoys for microRNAs (miRNAs) [5]. The human genome is estimated to encode approximately 15,000–17,000 lncRNAs, although the functions of most of these lncRNAs remain unclear. Recent studies have highlighted the involvement of deregulated lncRNAs in lung cancer initiation, progression, and therapy resistance [6]. Numerous dysregulated lncRNAs have been implicated in lung cancer, such as HOTAIR, H19, and MALAT1 [7,8], although the roles of many lncRNAs in oncogenesis remain unknown.

*Address for correspondence: Dr. Kuo-Wang Tsai,

Department of Research, Taipei Tzu Chi Hospital, Buddhist Tzu Chi Medical Foundation, 289, Jianguo Road, Xindian, Taipei, Taiwan.
E-mail: kwtsai6733@gmail.com

Supplementary material available online

Access this article online

Quick Response Code:



Website: www.tcmjmed.com

DOI: 10.4103/tcmj.TCMJ-D-25-00032

This is an open access article distributed under the terms of the Creative Commons Attribution-NonCommercial-NoDerivatives 4.0 License (CC BY-NC-ND), where it is permissible to download and share the work provided it is properly cited. The work cannot be changed in any way or used commercially without permission from the journal.

For reprints contact: WKHLRPMedknow_reprints@wolterskluwer.com

How to cite this article: Cheng CF, Tu YT, Chen YR, Lee MC, Ku HC, Tsai KW. Long noncoding RNA LOC441461 drives cancer growth and is associated with poor clinical outcomes. *Tzu Chi Med J* 2026;38(1):75-82.

LOC441461 is a 563-base pair lncRNA that shares a bidirectional promoter with the *STX17* gene on human chromosome 9 (coordinates: 99,886,317–99,906,601). According to Wang *et al.*, LOC441461 is upregulated in colorectal cancer tissues, and its high expression correlates with poor patient survival [9]. Interestingly, LOC441461 expression was found to be lower in primary colon tumors and liver metastases relative to normal mucosa, and LOC441461 knockdown reduced colon cancer cell proliferation by arresting the cancer cell cycle and inducing apoptosis [9]. By contrast, Lee *et al.* found that LOC441461 was downregulated in human gastric cancer and that its knockdown promoted cancer cell proliferation and metastasis [10]. Their findings suggest that LOC441461 may regulate transcriptional activity through interactions with several critical transcription factors. These contrasting findings indicate that LOC441461 may function differently depending on the cancer type. However, its role in lung cancer remains largely unexplored [10]. In this study, we investigated the clinical relevance of LOC441461 in lung cancer using public databases and explored its biological function through *in vitro* proliferation and cell cycle assays.

MATERIALS AND METHODS

Cell culture

The lung cancer cell lines A549, H1299, H1355, and CL1-5 and the human embryonic lung cell line HEL-299 were obtained from the American Type Culture Collection. All cells were cultured in Roswell Park Memorial Institute 1640 medium supplemented with 10% heat-inactivated fetal bovine serum (Invitrogen, Carlsbad, CA, USA).

LOC441461 expression according to the Cancer Genome Atlas data

The Cancer Genome Atlas (TCGA) project collects RNA expression data from both tumor and matched normal tissues obtained from hundreds of patients with lung cancer. In this study, we downloaded all level-3 RNA sequencing data for lung cancer from the TCGA Data Portal (<https://tcga-data.nci.nih.gov/tcga/dataAccessMatrix.htm>). These level-3 datasets contain processed expression values for each lncRNA, which have been derived through Illumina HiSeq sequencing. Specifically, we obtained expression profiles and corresponding clinical data for LUAD and LUSC. In addition, the expression levels of LOC441461 in human cancer were obtained and analyzed from the Gene Expression Profiling Interactive Analysis (GEPIA; <http://gepia.cancer-pku.cn/index.html>).

Extraction of RNA

Total RNA was extracted from tissue samples using TRIzol reagent (Invitrogen, Carlsbad, CA, USA) by following the manufacturer's protocol. Briefly, tissues were homogenized in 1 mL of TRIzol reagent, after which 0.2 mL of chloroform was added to separate the phases. RNA was then precipitated from the aqueous phase using 0.5 mL of isopropanol. The concentration, purity, and quantity of the extracted RNA were assessed using a NanoDrop 1000 spectrophotometer (NanoDrop Technologies Inc., USA).

Clinical samples

Thirty lung cancer tissues and corresponding adjacent normal samples were obtained from the Biobank of Taipei Tzu Chi Hospital, Taiwan. Informed consent was obtained from all patients by the Biobank of Taipei Tzu Chi Hospital. This study was conducted in accordance with the Declaration of Helsinki and approved by the ethics committee of Taipei Tzu Chi Hospital (14-IRB-042).

Real-time polymerase chain reaction

Complementary DNA was used for quantitative real-time polymerase chain reaction (PCR) analysis with LOC441461-specific primers. Gene expression was quantified using Fast SYBR Green Master Mix (Applied Biosystems; Thermo Fisher Scientific, Waltham, MA, USA). The expression level of LOC441461 was normalized to that of glyceraldehyde 3-phosphate dehydrogenase (GAPDH) using the ΔC_t method ($\Delta C_t = C_t_{\text{LOC441461}} - C_t_{\text{GAPDH}}$). The specific primers used in this study are listed in Supplementary Table 1.

siRNA transfection

In this study, LOC441461 expression was knocked down using siRNA oligonucleotide transfection. The detailed sequences are provided in Supplementary Table 1. A scrambled oligonucleotide was used as a negative control (NC), and all siRNAs were purchased from GenDiscovery Biotechnology (Taipei, Taiwan). Briefly, lung cancer cells were transfected with 10 nM siLOC441461 (siLOC441461#1, siLOC441461#2, or a pooled combination of siLOC441461#1 and siLOC441461#2) or scrambled control using Lipofectamine RNAiMAX reagent (Invitrogen; Thermo Fisher Scientific). Knockdown efficiency was assessed by real-time PCR.

Proliferation

A total of 2500 lung cancer cells were seeded into 96-well plates and transfected with siLOC441461 or a scrambled NC. Cell viability was measured at 0, 1, 2, and 3 days using the CellTiter-Glo One Solution Cell Proliferation Assay (Promega Corporation, Madison, WI, USA).

Colony formation assay

A total of 4000 cells were seeded into each well of a six-well plate and transfected with either si-LOC441461 or a scrambled NC using Lipofectamine RNAiMAX (Invitrogen; Thermo Fisher Scientific). After 3 days of incubation at 37°C, the culture medium was replaced with fresh medium, and the cells were further incubated for 10 days to allow colony formation. At the end of the incubation period, colonies were fixed with 4% formaldehyde for 2 min and stained with crystal violet solution (0.5% crystal violet, 5% formaldehyde, 50% ethanol, and 0.85% sodium chloride) for 2 h. After being air-dried, the wells were rinsed with distilled water. To quantify colony formation, the bound crystal violet dye was solubilized with 1 mL of 10% acetic acid in each well, and the absorbance was measured at 595 nm by using a spectrophotometer.

Cell cycle analysis

Lung cancer cells were transfected with siLOC441461 (a combination of siLOC441461#1 and siLOC441461#2) or a scrambled NC using Lipofectamine RNAiMAX reagent (Invitrogen; Thermo Fisher Scientific). After 48 h, 1×10^6 cells were harvested and fixed in 70% ethanol at -20°C overnight. The cells were then stained with 4',6-diamidino-2-phenylindole (ChemoMetec, Gydevang, Lillerød, Denmark) and analyzed with the NucleoView NC-3000 software (ChemoMetec).

Western blotting

Cells were harvested 48 h after transient transfection, washed with phosphate-buffered saline, and lysed in radioimmunoprecipitation assay buffer (50 mM Tris-HCl at pH 8.0, 150 mM NaCl, 1% NP-40, 0.5% sodium deoxycholate, and 0.1% sodium dodecyl sulfate) at 4°C for 30 min. Protein samples (40 μg per lane) were analyzed using sodium dodecyl sulfate–polyacrylamide gel electrophoresis; 10% or 12% polyacrylamide gel, then was transferred to membranes. The membranes were then blocked for 1 h at room temperature with blocking buffer (50 mM Tris-HCl at pH 7.6, 150 mM NaCl, 0.1% Tween-20, 5% nonfat dry milk, and 0.05% sodium azide) and incubated overnight at 4°C with the primary antibodies. After being washed, the membranes were incubated for 1 h at room temperature with the following HRP-conjugated secondary antibodies. After the membranes were washed three times with Tris-buffered saline containing 0.1% Tween-20, immunoreactive bands were visualized using the WesternBright ECL detection system (Advansta, Menlo

Park, CA, USA). The antibodies used in this study are listed in Supplementary Table 2.

Statistical analysis

Data from real-time PCR or the TCGA database were analyzed to examine the relative expression levels of LOC441461 in lung cancer cells. For the expression levels of LOC441461 in five lung cancer cell lines, a one-way ANOVA was performed to assess overall differences among the groups, followed by one-way ANOVA *post hoc* tests with Bonferroni correction to compare pairwise differences between each cell line. A $P < 0.05$ was considered statistically significant. Cumulative survival curves were drawn using the Kaplan–Meier method, and survival curves were compared using the log-rank test. For the cell proliferation assay, repeated measures ANOVA was used to evaluate the interaction between group and time. *Post hoc* pairwise comparisons between the two groups (N.C. vs. siLOC441461) at each time point (days 0, 1, 2, and 3) were conducted using ANOVA with Bonferroni correction. Cell proliferation and colony formation experiments were performed in triplicate. Histograms are used to present the mean values, and error bars indicate standard deviations. The data were analyzed using Student's *t*-test. Differences were considered significant if $P < 0.05$.

RESULTS

High LOC441461 expression in lung cancer is strongly associated with poor outcomes

In the present study, we examined LOC441461 expression in various human cancers. As shown in Figure 1, LOC441461

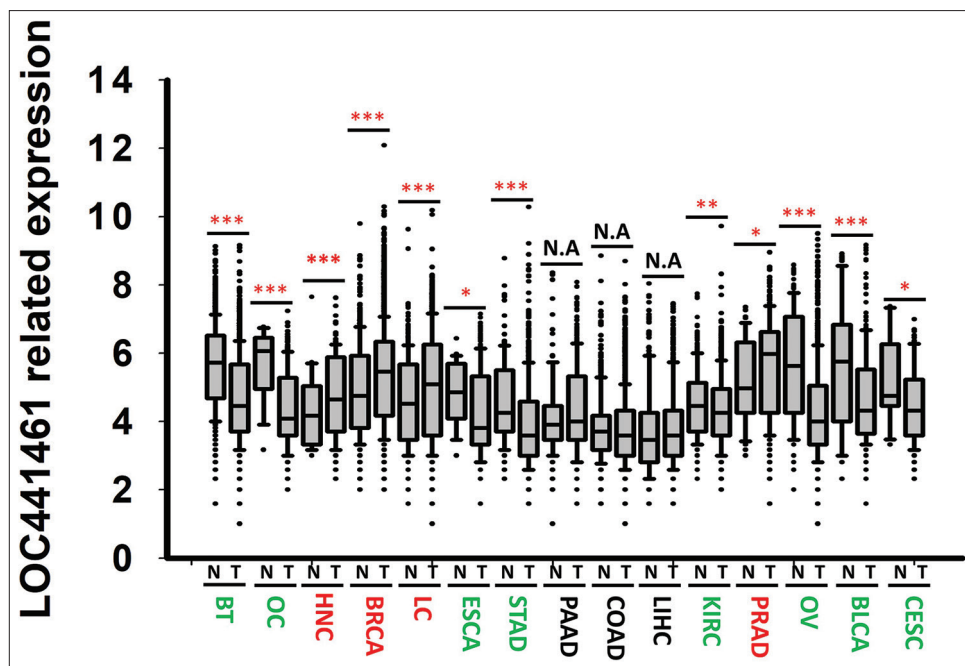


Figure 1: LOC441461 expression in human cancer cells according to GEPIA data. The expression levels of LOC441461 were analyzed across multiple human cancer types in comparison with their corresponding adjacent normal tissues, including brain tumor, oral cancer, head and neck cancer, breast cancer, lung cancer, esophageal cancer, stomach cancer, pancreatic cancer, liver cancer, kidney cancer, prostate cancer, ovarian cancer, bladder cancer, and cervical cancer. Green, red, and black indicate significant underexpression, significant overexpression, and no significant difference, respectively, of LOC441461 in tumor tissues relative to adjacent normal tissues. * $P < 0.05$; ** $P < 0.01$; *** $P < 0.001$. BT: brain tumor, OC: Oral cancer, HNC: Head and neck cancer, BRCA: breast cancer, LC: lung cancer, ESCA: Esophageal cancer, STAD: Stomach cancer, PAAD: Pancreatic cancer, COAD: colon cancer, LIHC: liver cancer, KIRC: kidney cancer, PRAD: prostate cancer, OV: ovarian cancer, BLCA: bladder cancer, and cervical cancer

was underexpressed in brain tumors ($P < 0.001$), oral cancer ($P < 0.001$), esophageal cancer ($P < 0.05$), stomach cancer ($P < 0.001$), kidney cancer ($P < 0.01$), ovarian cancer ($P < 0.001$), bladder cancer ($P < 0.001$), and cervical cancer ($P < 0.05$). By contrast, LOC441461 was markedly overexpressed in head and neck cancer ($P < 0.001$), breast cancer ($P < 0.001$), lung cancer ($P < 0.001$), and prostate cancer ($P < 0.05$). These findings suggest that LOC441461 may play cancer-type-specific roles in tumorigenesis. We further investigated the clinical relevance of LOC441461 for lung cancer prognosis using another independent datasets. TCGA data indicated that compared with that in normal tissue, LOC441461 expression was significantly higher in LUAD ($P < 0.001$) but nonsignificantly different in LUSC [$P = 0.76$; Figure 2a]. Real-time PCR analysis revealed that LOC441461 was significantly upregulated in LUAD compared with the corresponding adjacent normal tissues [$P < 0.001$; Figure 2b]. To examine the clinical impact of *LOC441461* expression in LUAD, we obtained detailed clinical information and expression data for *LOC441461* from the TCGA database. Using these data,

we evaluated the association of LOC441461 expression with overall survival (OS), progression-free survival (PFS), and disease-free survival (DFS) in these patients. A cutoff value for LOC441461 expression was determined through receiver operating characteristic curve analysis. On the basis of this cutoff, patients were divided into high and low LOC441461 expression groups. Kaplan–Meier survival analysis revealed that high LOC441461 expression had a significant association with poorer PFS ($P = 0.018$) and showed a trend toward associations with OS ($P = 0.081$) and DFS [$P = 0.051$; Figure 2c–e]. A univariate analysis indicated that high LOC441461 expression exhibited a similar trend toward poorer OS (hazard ratio [HR]: 1.31, 95% confidence interval [CI]: 0.97–1.76; $P = 0.082$) and DFS (HR: 1.53, 95% CI: 0.99–2.34; $P = 0.053$) and significant associations with shorter PFS [HR: 1.39, 95% CI: 1.06–1.84; $P = 0.019$; Table 1]. In multivariate analysis, high LOC441461 expression remained significantly associated with poorer PFS [adjusted HR: 1.45, 95% CI: 1.10–1.92; $P = 0.009$; Table 1]. A further analysis with data from an independent database validated these findings, indicating that high

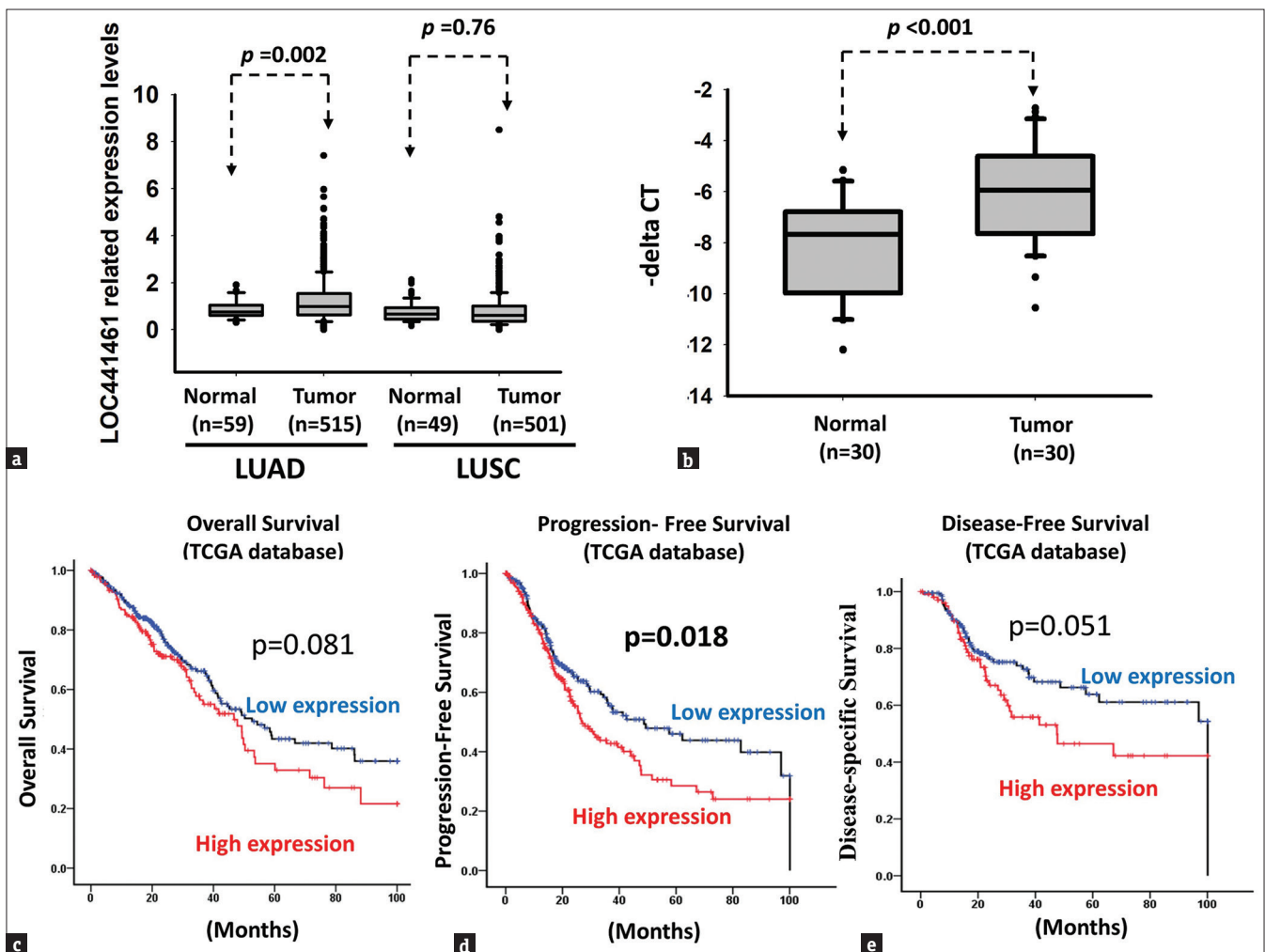


Figure 2: LOC441461 expression in human lung cancer cells according to TCGA data, (a) LOC441461 expression in lung adenocarcinoma (LUAD) and lung squamous cell carcinoma relative to that in adjacent normal tissue, (b) The expression levels of LOC441461 were analyzed in LUAD compared to corresponding adjacent normal tissues by real-time polymerase chain reaction. Correlations of LOC441461 expression with (c) overall survival, (d) progression-free survival, and (e) disease-free survival. LUAD: lung adenocarcinoma, LUSC: lung squamous cell carcinoma, CT: Computed tomography

LOC441461 expression was significantly correlated with poor OS (HR: 1.34, $P = 0.00019$) and PFS (HR: 1.29, $P = 0.026$), as shown in Supplementary Figure 1a and b. Collectively, these findings suggest that LOC441461 is significantly overexpressed in lung cancer. Thus, high LOC441461 expression may serve as a prognostic biomarker for poor outcomes in LUAD.

LOC441461 plays an oncogenic role in promoting the growth of lung cancer cells

The aforementioned findings indicate that LOC441461 is overexpressed in lung cancer and that high expression is correlated with poor survival and disease progression. However, the biological role of LOC441461 on lung cancer growth remains unclear. Thus, we examined the effects of LOC441461 knockdown on the growth and motility of lung cancer cells. We first determined the expression levels of LOC441461 in various lung cancer cells by using real-time PCR. According to the results, A549, H1299, and H1355 cells had higher LOC441461 expression compared with HEL299 cells [Figure 3a]. Furthermore, LOC441461 expression was predominantly localized in the cytoplasm of A549 and

H1299 cells [Supplementary Figure 2a and b]. Because A549 and H1299 cells had high LOC441461 expression, we selected them for further study. We transfected these cells with small interfering RNA (siRNA; siLOC441461#1 and siLOC441461#2) for 24 h and observed significantly lower LOC441461 expression in these cells relative to the expression in a NC group [Figure 3b and c]. We then assessed the biological function of A549 and H1299 cells with LOC441461 knockdown. As illustrated in Figure 3d, f and g, the cell proliferation and colony formation ability of the A549 cells were significantly lower after LOC441461 knockdown. Similarly, we observed that LOC441461 knockdown significantly inhibited H1299 cell proliferation and colony formation ability in the control group comparisons [Figure 3e-g].

LOC441461 regulates lung cancer cell growth by impairing cell cycle progression

The aforementioned results indicate that LOC441461 knockdown suppresses lung cancer cell proliferation and colony formation ability, including in A549 and H1299 cells [Figure 3]. We further analyzed the apoptosis

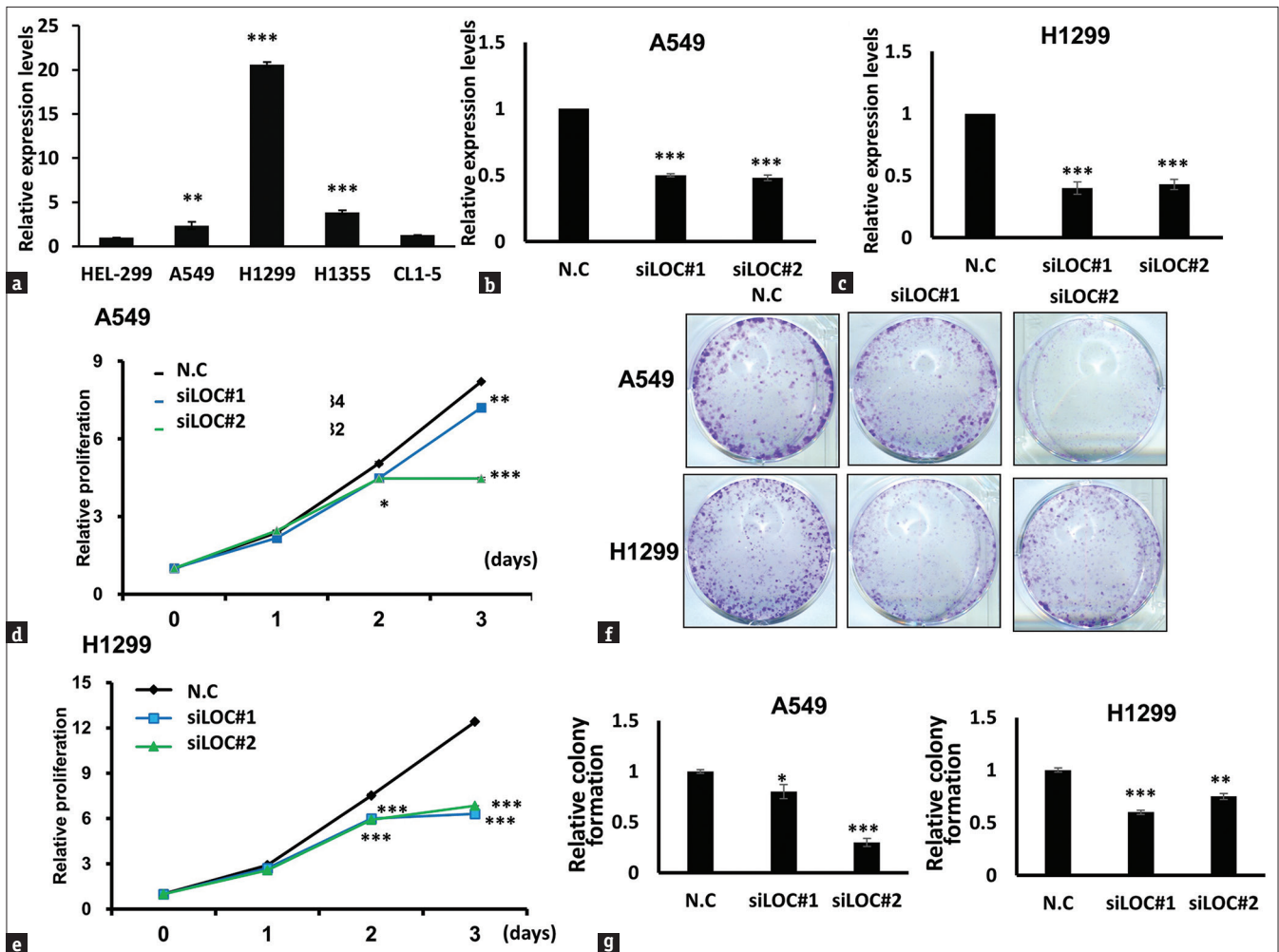


Figure 3: LOC441461 knockdown suppresses lung cancer cell growth, (a) Real-time polymerase chain reaction (PCR) results of LOC441461 expression in A549, H1299, H1355, and CL1-5 lung cancer cells and HEL-299 human embryonic lung cells. (b and c) Real-time PCR results of LOC441461 expression in A549 and H1299 cells after transfection with siLOC441461#1 and siLOC441461#2, respectively, (d and e) A549 and H1299 cell proliferation after LOC441461 knockdown, respectively, (f and g) A549 and H1299 colony formation after transfection with siLOC441461#1 and siLOC441461#2, respectively. All experiments were conducted in triplicate

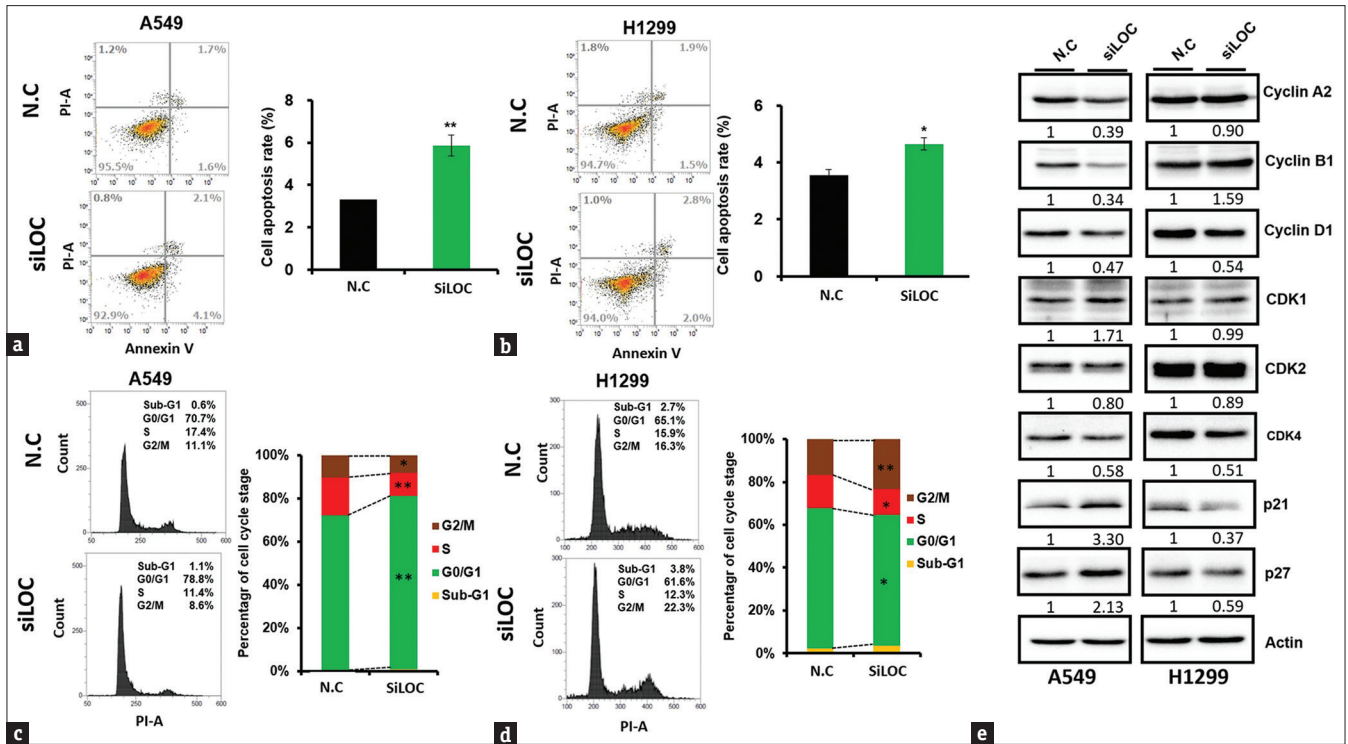


Figure 4: LOC441461 knockdown induced apoptosis and impaired cell cycle progression, (a and b) Prevalence of apoptosis in A549 and H1299 lung cancer cells; the cells were stained with propidium iodide and Annexin V and analyzed using an image flow assay. (c and d) Findings from flow cytometry assay on the distribution of cells in three phases of the cell cycle in A549 and H1299 cells with and without LOC441461 knockdown, (e) Western blot results for the expression of cell cycle-related genes in A549 and H1299 cells after LOC441461 knockdown for 48 h. The relative ratios of each band were quantified and are displayed below the panel. All experiments were conducted in triplicate

Table 1: Univariate and multivariate cox regression of associations of LOC441461 expression with overall survival, progression-free survival, and disease-free survival in 496 patients with lung adenocarcinoma

Characteristic	n (%)	OS			
		CHR (95% CI)	P	AHR (95% CI)	P
OS	n=496				
Low	311 (62.7)	1.00	0.082	1.00	0.084
High	185 (37.3)	1.31 (0.97–1.76)		1.31 (0.97–1.77)	
PFS					
Low	270 (54.4)	1.00	0.019	1.00	0.009
High	226 (45.6)	1.39 (1.06–1.84)		1.45 (1.10–1.92)	
DFS					
Low	191 (64.7)	1.00	0.053	1.00	0.063
High	104 (35.3)	1.53 (0.99–2.34)		1.51 (0.98–2.33)	

AHR were adjusted for AJCC pathological stage (II, III and IV VS. I). OS: Overall survival, PFS: Progression-free survival, DFS: Disease-free survival, CHR: Crude hazard ratio, AHR: Adjusted hazard ratio, CI: Confidence interval

and cell cycle progression of lung cancer cells with LOC441461 knockdown. As shown in Figure 4a and b, LOC441461 knockdown induced a modest but statistically significant increase in apoptosis in both cell lines compared with their respective control groups. These results indicate that LOC441461 involves in the growth of LUAD cells, although the magnitude of apoptosis induction was limited. In addition, we conducted an image flow assay and found that in A549 cells, siLOC441461 pool transfection was

associated with increased prevalence of the G0/G1 phase and significantly lower prevalence of the S and G2/M phases [Figure 4c]. However, in H1299 cells, siLOC441461 pool transfection was associated with decreased prevalence of the G0/G1 and S phases and increased prevalence of the G2/M phase [Figure 4d]. Thus, the effect of LOC441461 knockdown on cell cycle progression differed between A549 and H1299 cells. We further examined the expression levels of cell cycle-related genes in A549 and H1299 cells with LOC441461 knockdown. Our results indicated that in A549 cells, LOC441461 knockdown was associated with lower expression levels of CDK4 and cyclin A2, B1, and D1 and higher expression levels of p21 and p27 [Figure 4e]. However, in H1299 cells, only the expression levels of CDK4 and the cyclin D1 were lower after LOC441461 knockdown. Because A549 cells are p53 wild-type cells and H1299 cells are P53 null cells, this difference in the effect of LOC441461 knockdown between the two cell types might have stemmed from the p53 status of H1299 cells. However, the mechanism underlying this difference should be investigated in future studies.

DISCUSSION

Although our findings indicate that LOC441461 functions as a potential oncogenic factor in lung cancer by promoting cell cycle progression and inhibiting apoptosis, its expression pattern appears to differ between lung cancer subtypes. Analysis of TCGA data revealed that LOC441461 is

significantly overexpressed in LUAD but not in LUSC. These findings highlight the necessity of differentiating among cancer types when assessing LOC441461 expression and function in human malignancies. In colon cancer, LOC441461 was reported to be upregulated and associated with enhanced tumor cell proliferation and migration, indicating a tumor-promoting role [9]. This finding is consistent with our observations in LUAD, where LOC441461 knockdown suppressed proliferation and induced apoptosis. However, LOC441461 may play a tumor-suppressing role in gastric cancer. Low LOC441461 expression was found to be correlated with poor prognosis in gastric cancer, and LOC441461 knockdown increased the growth and motility of gastric cancer cells and exerted tumor-suppressing effects through the regulation of cell adhesion and genes related to the epithelial–mesenchymal transition [10].

In this study, we identified a novel oncogenic lncRNA, LOC441461, that is involved in the growth of LUAD cells. We also found that LOC441461 overexpression is associated with poor PFS in patients with LUAD. However, the exact mechanism through which LOC441461 promotes cell growth remains unclear. Our study showed that LOC441461 is primarily expressed in the cytoplasm, suggesting that it may regulate lung cancer cell proliferation by interacting with miRNAs to suppress the translation of tumor suppressor genes [9]. A previous study demonstrated that miR-335 suppresses the motility of metastatic breast cancer cells by regulating a set of genes, including SOX4 [11,12]. Gene expression omnibus (GDS3138) analysis revealed that LOC441461 expression was downregulated in lung metastatic breast cancer cells with miR-335 overexpression. Studies have indicated that miR-335 expression acts as a tumor suppressor in the inhibition of lung cancer cell growth and metastasis [13-16]. These studies' findings suggest that the miR-335-LOC441461 axis may regulate lung cancer cell growth by acting as a miR-335 sponge. However, further experiments are needed to fully elucidate the mechanism of LOC441461.

Interestingly, our findings demonstrate that the effects of LOC441461 knockdown on cell cycle progression and apoptosis differ for A549 (p53 wild-type) versus H1299 (p53-null) cells, suggesting the existence of some mechanisms that do not depend on p53 status and other mechanisms that do. Other research has revealed that p53 status directly leads to drug-treatment-induced cell arrest by regulating p21 expression [17,18]. In A549 cells, LOC441461 knockdown significantly upregulated the expression of the cyclin-dependent kinase inhibitors p21 and p27 and reduced the levels of CDK4 and the cyclin D1, A2, and B1 [Figure 4]. These changes were associated with G0/G1 cell cycle arrest, increased apoptosis, and p21 expression [19]. Given that p21 is a direct transcriptional target of p53, our findings imply that LOC441461 may negatively regulate the p53 signaling pathway. Upon LOC441461 silencing, p53 activity is likely to be restored, leading to enhanced p21-mediated cell cycle inhibition and apoptotic induction. By contrast, in H1299 cells lacking functional p53, LOC441461 knockdown did not alter p21 or p27 expression but still reduced CDK4 and cyclin

D1 levels. Interestingly, these cells were more likely to be in the G2/M phase and to undergo apoptosis, indicating a p53-independent mechanism of G2/M arrest. This suggests that LOC441461 may also regulate cell cycle progression through other pathways, potentially involving mitotic regulators such as PLK1, CDC25C, or aurora kinases. The observed apoptosis in the two cell lines following LOC441461 depletion underscores the potential oncogenic role of LOC441461 in LUAD.

CONCLUSION

Overall, our findings reveal that LOC441461 contributes to LUAD cell proliferation by modulating cell cycle regulators and apoptosis through p53-dependent and p53-independent pathways. Targeting LOC441461 may represent a promising therapeutic strategy for LUAD regardless of p53 status.

Acknowledgments

The authors appreciate the assistance of Biobank of Taipei Tzu Chi Hospital for the processing of clinical specimens. The authors would also like to thank the Core Laboratory, Department of Research, Taipei Tzu Chi Hospital, Buddhist Tzu Chi Medical Foundation, for technical support and the use of their premises.

Data availability statement

The datasets generated during and/or analyzed during the current study are available from the corresponding author on reasonable request.

Financial support and sponsorship

This work was supported by the National Science and Technology Council (113-2314-B-303-014 and 114-2314-B-016), Taipei Tzu Chi Hospital and Buddhist Tzu Chi Medical Foundation (TCRD-TPE-MOST-111-15 and TCMF-CM3-112-03), and through collaboration between Tzu Chi Hospital and Academia Sinica (TCAS-112-02).

Conflicts of interest

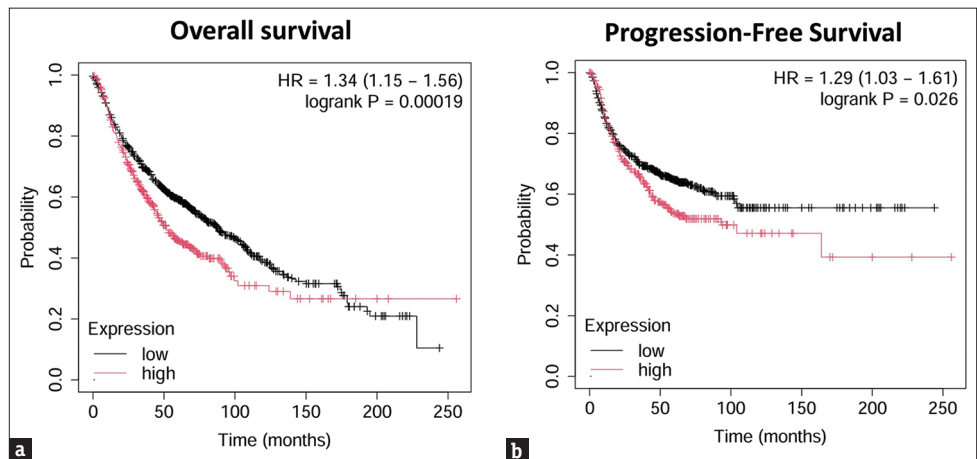
Dr. Ching-Feng Cheng, an editorial board member at *Tzu Chi Medical Journal*, had no role in the peer review process of or decision to publish this article. The other authors declared no conflicts of interest in writing this paper.

REFERENCES

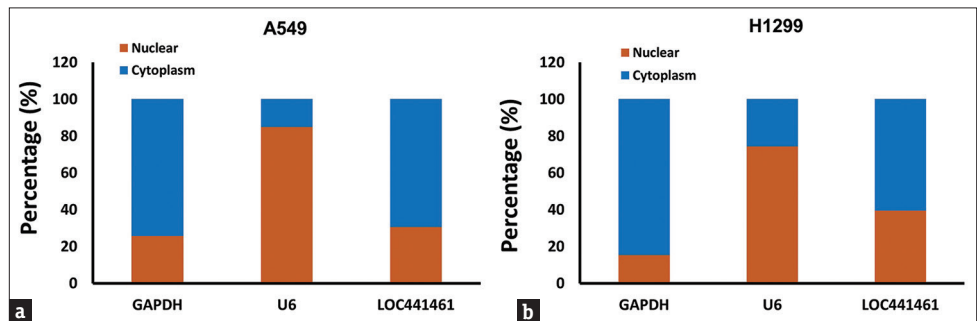
- Schabath MB, Cote ML. Cancer progress and priorities: Lung cancer. *Cancer Epidemiol Biomarkers Prev* 2019;28:1563-79.
- Filho AM, Laversanne M, Ferlay J, Colombet M, Piñeros M, Znaor A, et al. The GLOBOCAN 2022 cancer estimates: Data sources, methods, and a snapshot of the cancer burden worldwide. *Int J Cancer* 2025;156:1336-46.
- Socinski MA, Crowell R, Hensing TE, Langer CJ, Lilenbaum R, Sandler AB, et al. Treatment of non-small cell lung cancer, stage IV: ACCP evidence-based clinical practice guidelines (2nd edition). *Chest* 2007;132:277S-89S.
- Hanahan D, Weinberg RA. The hallmarks of cancer. *Cell* 2000;100:57-70.
- Gugnoni M, Kashyap MK, Wary KK, Ciarrocchi A. lncRNAs: The unexpected link between protein synthesis and cancer adaptation. *Mol Cancer* 2025;24:38.
- Bridges MC, Daulagala AC, Kourtidis A. LNCcation: lncRNA localization and function. *J Cell Biol* 2021;220:e202009045.
- Zhao X, Jin X, Zhang Q, Liu R, Luo H, Yang Z, et al. Silencing of the

- lncRNA H19 enhances sensitivity to X-ray and carbon-ions through the miR-130a-3p/WNK3 signaling axis in NSCLC cells. *Cancer Cell Int* 2021;21:644.
8. Xia S, Lu X, Wang W, Pan X, Cui J, Wang S, et al. The regulatory role and therapeutic potential of long non-coding RNA in non-small cell lung cancer. *J Cancer* 2025;16:1137-48.
 9. Wang JH, Lu TJ, Kung ML, Yang YF, Yeh CY, Tu YT, et al. The long noncoding RNA LOC441461 (STX17-AS1) modulates colorectal cancer cell growth and motility. *Cancers (Basel)* 2020;12:3171.
 10. Lee SS, Park J, Oh S, Kwack K. Downregulation of LOC441461 promotes cell growth and motility in human gastric cancer. *Cancers (Basel)* 2022;14:1149.
 11. Tavazoie SF, Alarcón C, Oskarsson T, Padua D, Wang Q, Bos PD, et al. Endogenous human microRNAs that suppress breast cancer metastasis. *Nature* 2008;451:147-52.
 12. Png KJ, Yoshida M, Zhang XH, Shu W, Lee H, Rimmer A, et al. MicroRNA-335 inhibits tumor reinitiation and is silenced through genetic and epigenetic mechanisms in human breast cancer. *Genes Dev* 2011;25:226-31.
 13. Wang X, Xiao H, Wu D, Zhang D, Zhang Z. miR-335-5p regulates cell cycle and metastasis in lung adenocarcinoma by targeting CCNB2. *Oncotargets Ther* 2020;13:6255-63.
 14. Liu J, Bian T, Feng J, Qian L, Zhang J, Jiang D, et al. miR-335 inhibited cell proliferation of lung cancer cells by target Tra2 β . *Cancer Sci* 2018;109:289-96.
 15. Gong M, Ma J, Guillemette R, Zhou M, Yang Y, Yang Y, et al. miR-335 inhibits small cell lung cancer bone metastases via IGF-IR and RANKL pathways. *Mol Cancer Res* 2014;12:101-10.
 16. Du W, Tang H, Lei Z, Zhu J, Zeng Y, Liu Z, et al. miR-335-5p inhibits TGF- β 1-induced epithelial-mesenchymal transition in non-small cell lung cancer via ROCK1. *Respir Res* 2019;20:225.
 17. Yuan L, Zhang Y, Xia J, Liu B, Zhang Q, Liu J, et al. Resveratrol induces cell cycle arrest via a p53-independent pathway in A549 cells. *Mol Med Rep* 2015;11:2459-64.
 18. Tseng YH, Tran TT, Tsai Chang J, Huang YT, Nguyen AT, Chang IY, et al. Utilizing TP53 hotspot mutations as effective predictors of gemcitabine treatment outcome in non-small-cell lung cancer. *Cell Death Discov* 2025;11:26.
 19. Waldman T, Kinzler KW, Vogelstein B. p21 is necessary for the p53-mediated G1 arrest in human cancer cells. *Cancer Res* 1995;55:5187-90.

SUPPLEMENTARY MATERIAL



Supplementary Figure 1: Clinical effects of LOC441461 expression in lung cancer according to GENT data. Correlations of LOC441461 with (a) overall survival and (b) progression-free survival. HR: Hazard ratio



Supplementary Figure 2: Subcellular localization analysis of LOC441461 in lung cancer cell lines. After nuclear and cytoplasmic fractionation, total RNA from A549 (a) and H1299 (b) cells was extracted and subjected to reverse transcription followed by real-time polymerase chain reaction (PCR). GAPDH was used as a cytoplasmic marker, and U6 as a nuclear marker. The expression levels of LOC441461 in the nuclear and cytoplasmic fractions were quantified separately by real-time PCR

Supplementary Table 1: The sequence of primers and siRNA used in this study

Primer	5'~3'
GAPDH-F	TGCACCACCAACTGCTTAGC
GAPDH-R	GGCATGGACTGTGGTCATGAG
LOC441461-F	TGATAAGCTGTTAAACCAGAACCG
LOC441461-R	GGCAACATTTCAGTCCAGTG
siRNA	CTCGCTTCGGCAGCACA
si-LOC441461#1	Sense: 5'-GGAACUGAAAUGUUGCCUUTT-3' Antisense: 5'-AAGGCAACAUUUCAGUUCCTT-3'
si-LOC441461#2	Sense: 5'-GCUGCUACAUAACUGAUUTT-3' Antisense: 5'-AAUCAGUUAUGUAGCAGCTT-3'

Supplementary Table 2: The antibodies used in this study

Antibody name	1 st Ab dilution	MW (kDa)	Company	Host	2 nd Ab dilution
CDK1	1:200	34, 27	10762-1-AP, proteintech	Rabbit	1:5000
CDK4	1:1000	34	MA5-12984, ThermoFisher	Mouse	1:5000
CDK2	1:1000	34	MA5-17052, ThermoFisher	Mouse	1:5000
CyclinA2	1:500	56	18202-1-AP, proteintech	Rabbit	1:5000
CyclinB1	1:500	55-60	55004-1-AP, proteintech	Rabbit	1:5000
CyclinD1	1:200	36	MA5-16356, ThermoFisher	Rabbit	1:5000
P21	1:1000	21	#2947, Cell signaling Technology, Inc., USA	Rabbit	1:5000
P27	1:500	27	25614-1-AP, proteintech	Rabbit	1:5000
β -actin (ACTB)	1:5000	43	MAB1501, Millipore	Mouse	1:5000

MW: Molecular weight